Available online at www.sciencedirect.com
SCIENCE DIRECT®

Journal of Molecular Catalysis A: Chemical 218 (2004) 133–140

JOURNAL OF MOLECULAR CATALYSIS A: CHEMICAL

www.elsevier.com/locate/molcata

The effect of iron on the adsorption properties of $CuMnZrO_2$ catalysts studied by temperature-programmed desorption and FTIR spectroscopy

Run Xu, Zhong-yi Ma, Cheng Yang, Wei Wei, Wen-huai Li, Yu-han Sun*

State Key Laboratory of Coal Conversion, Institute of Coal Chemistry, Chinese Academy of Sciences, 27 South Taoyuan Road, Taiyuan 030001, PR China

Received 23 December 2003; received in revised form 12 April 2004; accepted 12 April 2004

Abstract

The adsorption of CO on the precipitated Fe-$CuMnZrO_2$ catalysts for mixture alcohols synthesis were investigated using temperature-programmed desorption and FTIR spectra recorded at adsorption temperature in the range 298–673 K, in order to detect any synergy in the adsorption of CO on $CuMnZrO_2$ as a result of iron addition. In the case of $CuMnZrO_2$ catalyst, only one kind of CO adsorbed or desorbed, which was ascribed to weakly adsorbed CO species on copper sites, was detected in FTIR and TPD study. Moreover, for $CuMnZrO_2$ catalyst the formation of bidentate carbonate species was favored at 298 K, and bicarbonate species formed at higher temperature. When iron was introduced in $CuMnZrO_2$ catalyst, it was found that the adsorption features of catalysts changed significantly. The presence of iron improved the copper dispersion, which resulted in increasing of the total adsorption of CO, and intensified the reaction between CO and catalyst surface. Several kinds of CO adsorbed or desorbed were detected on Fe-$CuMnZrO_2$. The formation of bicarbonate species took place at 298 K, and formate species was detected at higher temperature, suggesting that the presence of iron greatly influenced the process of methanol synthesis.

Keywords: Cu/ZrO_2 catalyst; Higher alcohols synthesis; Iron effect; CO adsorption; DRIFT; TPD

1. Introduction

Higher alcohols synthesis from coal or natural gas via syngas due to its potential application as a good gasoline blend or alternative motor fuel for the reduction of exhaust emission has resulted in significant research. As a result, several catalytic systems for higher alcohol synthesis through CO hydrogenation were developed [1,2].

Copper-containing catalysts, such as Cu/ZnO, Cu/Al_2O_3 and Cu/SiO_2, have been intensely studied because of their activity in the CO and CO_2 hydrogenation. In the last few decades, many papers have centered on the characterization of Cu/ZrO_2-based catalysts because it showed a good activity for methanol synthesis [3,4]. The controversy concerning the nature of the surface intermediate, which was pivotal to the formation of methanol, was well known. Indeed, for many authors the formate species was the precursor of methanol [5–9], whereas others [10–12] considered that formate was not the precursor of methanol and that it was rather the bidentate carbonate which was hydrogenated to the methoxy species. It was possible that the nature of the pivotal species depended on the nature of the support. However, the conclusions were admitted for most researchers: zirconia provided adsorption sites for the reactive intermediates, and the formation of intermediate species could be varied by doping different promoters.

In our previous work, it was found that certain proportion for higher alcohols was obtained over iron, cobalt and nickel modified Cu/ZrO_2-based methanol synthesis catalysts [13–15]. Furthermore, the presence of iron in $CuMnZrO_2$ catalyst greatly enhanced the formation of higher alcohols, which were a mixture of straight chain alcohols and branched alcohols (mainly isobutanol). Under the reaction conditions of 573 K, 8.0 MPa and 8000 h^{-1}, the alcohols space-time-yield was up to 0.424 $g\,ml^{-1}\,h^{-1}$, but the methanol content in the alcohols product was relatively high. Increase of C_2^+ alcohols is desirable from the practical point of view. The effect of iron on the structural and physical properties of the copper species in the catalysts was discussed in our earlier reports [16,17]. It was found that

---

* Corresponding author. Tel.: +86-351-4049612; fax: +86-351-4041153.
E-mail address: yhsun@sxicc.ac.cn (Y.-h. Sun).

1381-1169/$ – see front matter © 2004 Elsevier B.V. All rights reserved.
doi:10.1016/j.molcata.2004.04.013

a stronger interaction between copper and iron took place, which was favorable for chain growth to produce higher alcohols. In the present work, the interaction of CO with $CuMnZrO_2$ or Fe-$CuMnZrO_2$ catalysts were investigated by temperature-programmed desorption and in situ diffuse reflectance FTIR in order to provide an insight into the effect of iron on the nature of adsorbed species on the surface.

2. Experimental

2.1. Preparation of catalysts

$CuMnZrO_2$ catalysts were prepared by co-precipitation of a solution of $Cu(NO_3)_2 \cdot 3H_2O$, $Mn(NO_3)_2$, and $ZrOCl_2 \cdot 8H_2O$ with an aqueous solution of Na_2CO_3 at 343 K and a constant pH of 10 in a well-stirred thermo-stated container. Then the precipitates were aged at 343 K for 2 h. After washed thoroughly with distilled water, the precipitates were dried at 393 K for 12 h, and then calcined at 623 K in air for 3 h. Fe-$CuMnZrO_2$ catalysts were prepared using the same procedures as for $CuMnZrO_2$, except that $Fe(NO_3)_3 \cdot 9H_2O$ was introduced into the mixed solutions. The composition of the prepared catalysts was as follows: Cu:Mn:Zr:Fe = 1:0.5:2:0.1 (molar ratio).

2.2. Characterization of catalysts

The BET surface areas of catalysts were determined by N_2 adsorption at 77 K using the Tristar 3000 Chemical Adsorption Instrument (Micromeritics). Powder X-ray diffraction (XRD) patterns were recorded on a Rigaku D/Max diffractorments with a Cu target and Ni filter.

The Cu surface area (S_{Cu}) was determined by applying a N_2O pulse method as described by Evans et al. [18]. A catalyst sample was placed in a quartz tube reactor and reduced in flowing H_2 (99.99%). After reduction, the gas flow was switched to Ar (99.99%) and the temperature was lowered to 353 K. A pulse of N_2O (99.995%) was introduced into the argon flow by means of a calibrated sample valve. The exit gas was analyzed by mass spectrometer (QMS, Balzers OmniStar 200). The amount of surface Cu was calculated from the amount of nitrogen evolved, assuming the dissociation of N_2O takes place on surface Cu followed the equation (average atom density: 1.49×10^{19} atoms/m^2):

$$N_2O(g) + 2Cu_s = N_2(g) + (Cu\text{–}O\text{–}Cu)_s \quad (1)$$

X-ray adsorption spectra (XAFS) around the Cu K-adsorption edge were obtained using the deamline of 4W1B of Beijing Synchrotron Radiation Facility (BSRF). The storage ring was operated at 2.2 GeV with a typical current of 50 mA. The fixed-exit Si(1 1 1) flat double crystals were used as monochromator. The EXAFS data were processed with the National Synchrotron Radiation Laboratory analysis programs (NSRLXAFS). A total of 4.0 nearest oxygen was found for each copper site at an average distance of 0.195 nm on the bulk CuO and these results were in good agreement with the conclusion of crystal analysis, which indicated that the fixed error in our experimentation and data analysis was very low.

The temperature-programmed desorption (TPD) experiments were carried out on a flow apparatus and the isothermal adsorption of CO was used prior TPD. The sample (200 mg) was reduced in a quartz micro reactor according to the following pre-treatment: H_2 (573 K, 6 h) → Ar (573 K, 0.5 h) → Ar (298 K). Afterwards, isothermal adsorption of CO was performed at temperatures between 298 and 573 K by injecting the CO/Ar (5 vol.% CO) mixture gas until the catalyst surface was saturated. After cooling to room temperature in CO/Ar mixture gas, the weakly adsorbed CO species was swept with pure Ar. The total amount of CO adsorption could be calculated from the adsorption curve and remove curve. Subsequently, the TPD experiments were carried out. The temperature of the system was raised linearly ($10\,K\,s^{-1}$ in general in present work) under an Ar gas flow. The analysis of the effluent gases was performed with a mass spectrometer (QMS, Balzers OmniStar 200). MS signals at $m/z = 28$ (CO), and 44 (CO_2) were continuously recorded. All spectra recorded from desorption were referenced to those of corresponding blank samples. The CO peaks were corrected for fragmentation of CO_2 ($CO_2 \rightarrow CO + O$) in the spectrometer.

The diffuse reflectance FTIR (DRIFT) spectra were recorded using Nicolet Magna-II 550 FTIR spectrometer equipped with Spectra-Tech Diffuse Reflectance Accessory and a high temperature in situ cell with ZnSe windows. A KBr beam splitter has been used with a TGS detector. One set of stainless steel gas lines was built and connected to the cell. This allowed in situ measurements for adsorption in a flow of gas. The catalyst was reduced according to the following pre-treatment: H_2 (573 K, 6 h) → Ar (573 K, 0.5 h) → Ar (298 K). After that, the catalyst was exposed to CO (99.999%) for 1 h at 298 K and purged with Ar to remove gaseous CO, and the IR spectra were recorded. Then, the temperature of system was increased to other desired value (between 298 and 673 K) in Ar. After adsorbed CO at this temperature, the catalyst was cooled down in CO to room temperature, swept with Ar and collected the IR spectra. Subsequently, the above-mentioned experiments procedure was applied again.

3. Results and discussion

3.1. Textural and structural properties of Fe-$CuMnZrO_2$ catalysts

The surface area measurements for catalysts were listed in Table 1. $CuMnZrO_2$ catalyst showed large surface area with the average pore size of 3.3 nm. The addition of iron could slightly increase the surface area and enlarge the pore size.

Table 1
Texture parameters and copper dispersion of various catalysts

Sample	S_{BET} ($m^2 g^{-1}$)	r_P (nm)	V_P ($mL g^{-1}$)	S_{Cu} ($m^2 g^{-1}$)	D_{Cu} (%)
$CuMnZrO_2$	193	3.3	0.16	6.32	5.7
$Fe\text{-}CuMnZrO_2$	196	4.0	0.20	7.15	6.6

S_{Cu}: copper surface area; D_{Cu}: dispersion of copper.

Similar to $CuMnZrO_2$, Fe-modified catalysts hardly showed the obvious XRD patterns, suggesting that the components were highly dispersed and the zirconia were amorphous. However, measured by N_2O titration, the Cu surface area and dispersion increased obviously due to the addition of iron (see Table 1). Likewise results from the EXAFS experiments were presented in Table 2. Compared to $CuMnZrO_2$ catalyst, the coordination number of $Fe\text{-}CuMnZrO_2$ decreased and the distance of Cu–O slightly enhanced. This revealed that the Cu species existed in much smaller crystallites and exhibited an amorphous-like or less well-ordered structure feature. In this case, the very high Debye–Waller factors associated with this shell also indicated the presence of great disorder. Therefore, these results demonstrated that the iron both as a support promoter influenced the texture of catalyst and as an additive enhanced the dispersion of Cu.

3.2. Isothermal adsorption of CO

The isothermal adsorption of CO was measured at different temperatures (see Fig. 1), and then the total amount of CO adsorption was listed in Table 3. When the CO adsorption on $CuMnZrO_2$ catalyst was carried out at 298 K, the total 498 $\mu mol\, g^{-1}$ of CO were adsorbed and no other gases were evolved during this adsorption. The similar phenomenon was observed on the isothermal adsorption of CO at 373 K except that there was a delay in the appearance of CO, which indicated that the uptake of CO increased. Furthermore, CO_2 was detected for the isothermal adsorption of CO at 473 K when the adsorption of CO was saturated. It suggested that the CO dissociation or the disproportionation reaction took place on the catalyst surface at present condition. As the temperature reached to 573 K, the adsorption of CO need a long time to get saturated and CO_2 was evolved during the isothermal contact CO, suggesting that the reaction of CO with the catalyst was intensified due to the rise of adsorption temperature. The spectra of the isothermal adsorption of CO on the Fe modified catalyst were similar to that on $CuMnZrO_2$ catalyst besides the CO uptake obviously increased (see Fig. 2). Moreover, the amount of desorbed CO_2 increased obviously at higher adsorption temperature compared with $CuMnZrO_2$. This indicated that iron could increase the adsorption of CO over catalyst and improve the reaction between CO and catalyst surface.

Table 2
Fitting results of CuO EXAFS for Cu–O band

Sample	Shell	Coordination number	Shell radius (nm)	Debye–Waller factors ($10^{-2}\, nm^{-1}$)
CuO	Cu–O	4.00	0.195	–
$CuMnZrO_2$	Cu–O	3.62	0.197	0.44
$Fe\text{-}CuMnZrO_2$	Cu–O	3.50	0.198	0.51

Fitting range in κ-space: 0.2–1 nm^{-1} with the weight of κ^3.

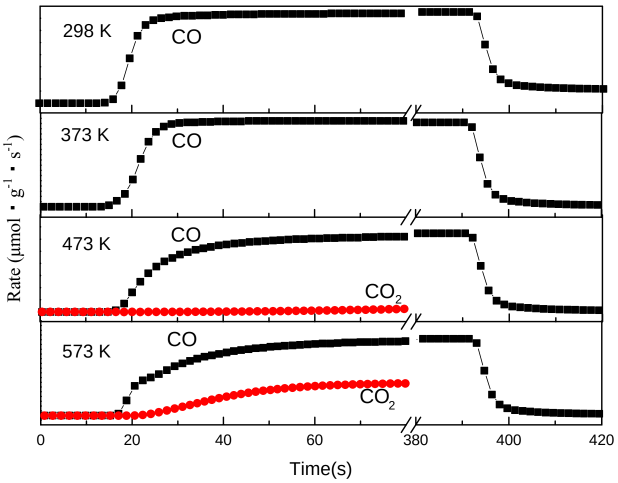

Fig. 1. Isothermal adsorption of CO on $CuMnZrO_2$ catalysts.

3.3. CO temperature-programmed desorption

Fig. 3 gave the spectra of CO-TPD after isothermal adsorption on $CuMnZrO_2$ catalysts at different temperatures. When the CO adsorption on $CuMnZrO_2$ catalyst was carried out at 298 K, CO_2 was the major product with the desorption peak at 506 K and a hump at 651 K (see Fig. 3A), while only a small amount of CO was evolved at 343 K. With the CO adsorption at 373 K, the large amount of CO_2 was released and appeared four peaks at 352, 414, 490 and 654 K, respectively, while the desorption of CO shifted to

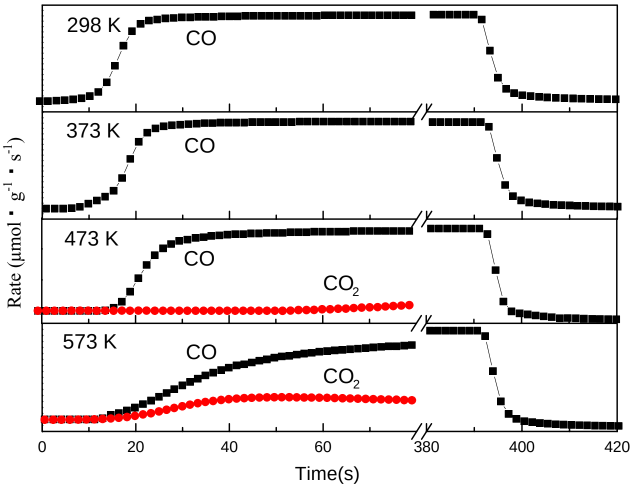

Fig. 2. Isothermal adsorption of CO on $Fe\text{-}CuMnZrO_2$ catalysts.

Table 3
CO-TPD of $CuMnZrO_2$ and Fe-$CuMnZrO_2$ catalysts

Temperature of CO adsorption (K)	$CuMnZrO_2$			Fe-$CuMnZrO_2$			
	CO_{ads} [a]	CO_{des}	CO_{2des}	CO_{ads}	$CO_{\alpha des}$	$CO_{\beta des}$	CO_{2des}
298	498	36	311	525	35	7	288
373	893	40	644	935	52	61	470
473	1031	67	651 (15[b])	1129	81	155	531 (26)
573	1364	30	921 (33)	1432	51	167	570 (107)

[a] The unit was $\mu mol\,g^{-1}$.
[b] The amount of CO_2 desorption during isothermal adsorption.
CO_{ads}, the total amount of CO adsorption, CO_{des}, the amount of CO desorption, CO_{2des}, the amount of CO_2 desorption.

336 K (see Fig. 3B). When the adsorption temperature further increased to 473 and 573 K, the amount of desorbed CO_2 increased regularly (see Fig. 3C and D). In principle, as the adsorption temperature increased the amount of desorbed CO reached a maximum at 473 K and then decreased, while the CO_2 increased monotonous.

Fig. 4 gave the spectra of CO-TPD on Fe-$CuMnZrO_2$ catalysts after isothermal adsorption at different temperatures. Fe-$CuMnZrO_2$ catalyst showed two CO desorption peaks appeared at 343 and 402 K, corresponding to the adsorption of CO on copper sites and modified iron sites, respectively. Moreover, it was noteworthy that the peak of CO desorbed from iron sites increased continually and shifted to high temperature simultaneously with the rise of adsorption temperature.

Over Cu/Al_2O_3 catalysts, Robinson and Mol [19] observed that CO desorbed in temperature range of 313–623 K with two distinct peaks. The peak at low temperature was ascribed to the weakly adsorbed CO species on copper sites and another peak was ascribed to the strongly adsorbed CO species on copper sites. However, we only observed one peak at 336–343 K and detected several peaks of desorbed CO_2 in higher temperature range. The difference might be related to the conversion of strongly adsorbed CO on catalyst

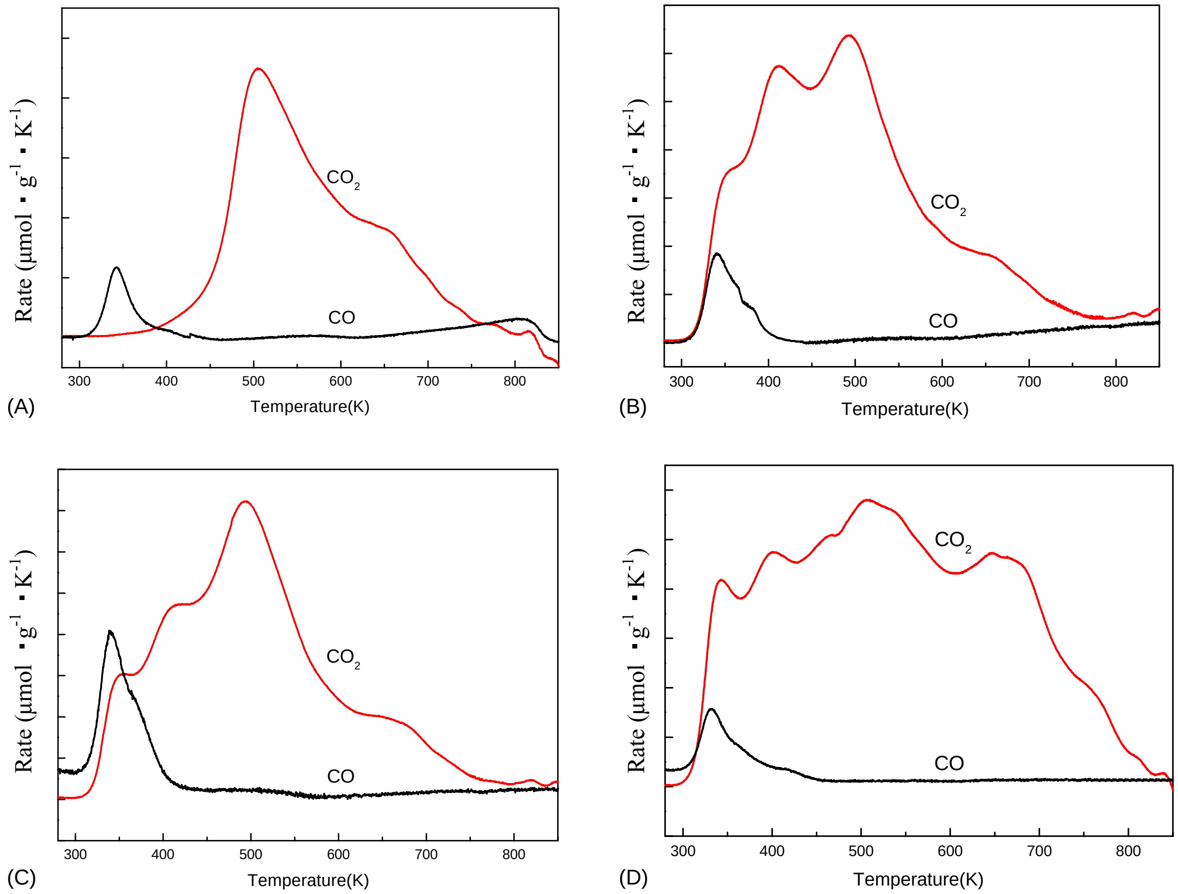

Fig. 3. TPD spectra after isothermal adsorption of CO on $CuMnZrO_2$ catalysts at different temperatures: (A) 298 K; (B) 373 K; (C) 473 K; (D) 573 K.

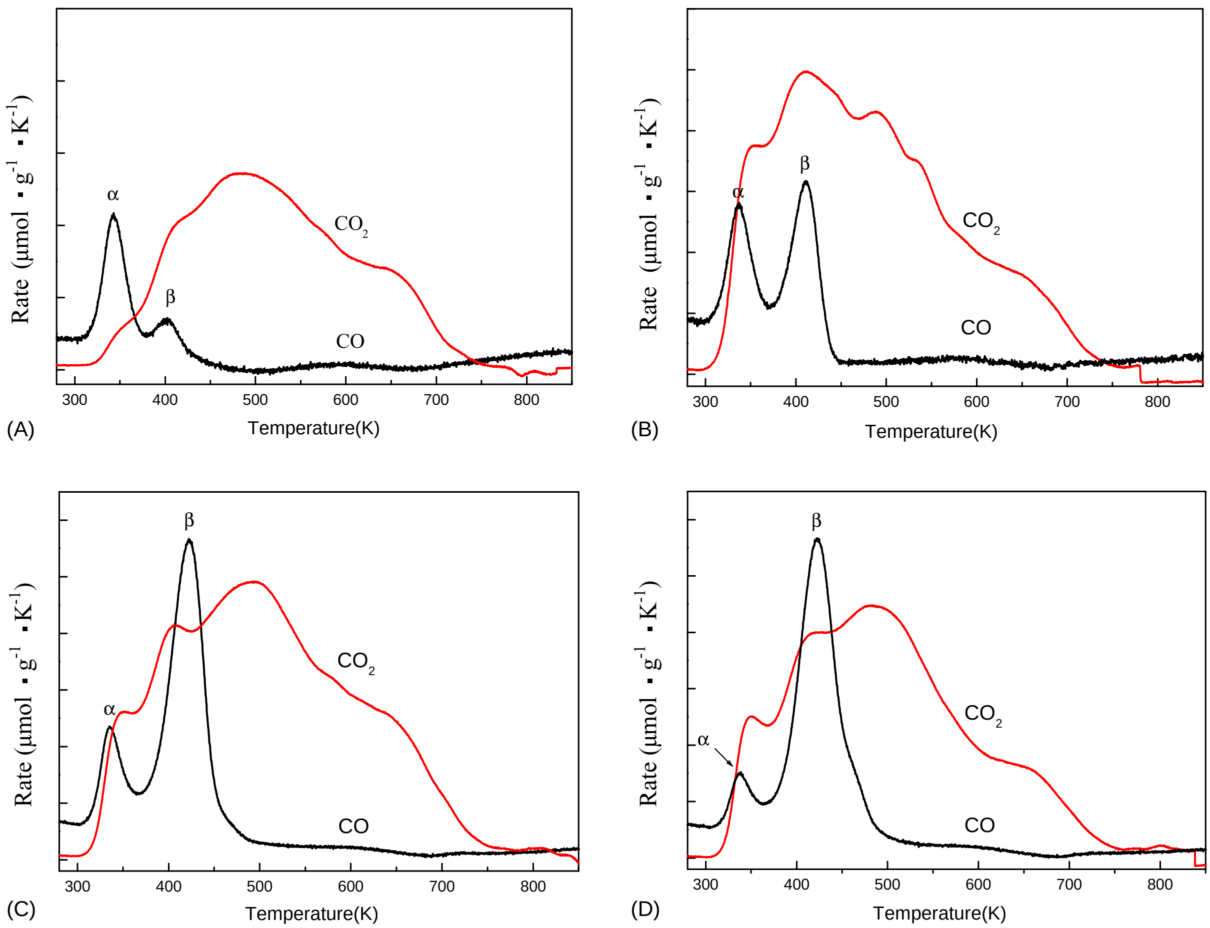

Fig. 4. TPD spectra after isothermal adsorption of CO on Fe-CuMnZrO_2 catalysts at different temperatures: (A) 298 K; (B) 373 K; (C) 473 K; (D) 573 K.

to some species at higher desorption temperature, which decomposed and released the large amount of CO_2 at the corresponding temperature.

The amounts of adsorbed CO and that of desorbed CO and CO_2 during the experiments were listed in Table 3 in detail. It could be seen that the total uptake of CO and desorption of CO_2 increased with the rise of adsorption temperature both on CuMnZrO_2 and Fe-CuMnZrO_2 catalyst. However, the amount of CO desorbed from copper sites showed a maximum at 473 K, while the CO desorbed from iron sites increased continually.

It was noteworthy that the remaining carbon ($CO_{ads} - CO_{des} - CO_{2des}$) on catalyst surface coming from disproportionation reaction or the dissociation desorption of CO increased with the rise of adsorption temperature and iron obviously enhanced the reaction. For instance, the remaining carbon was 151 μmol g^{-1} (498 − 36 − 311) for CuMnZrO_2 catalyst at 298 K, and was 380 μmol g^{-1} (1364 − 30 − 921 − 33) at 573 K. Correspondingly, for the Fe-CuMnZrO_2 catalysts it was 195 μmol g^{-1} (525 − 35 − 7 − 288) at 298 K and 537 μmol g^{-1} (1432 – 51 – 167 – 570 – 107) at 573 K. It clearly indicated that the presence of iron improved the disproportionation reaction or the dissociation desorption of CO on catalyst.

Apparently, the CO_2 desorption was suppressed at the presence of iron during TPD process. In general, CO_2 could result from the disproportionation reaction ($2CO \rightarrow CO_2 + C$), the dissociation desorption of CO, the decomposition of carbonaceous species or the interaction of CO with lattice oxygen [20]. Disproportionation reaction or the dissociation desorption of CO could take place at low temperature, as revealed by the spectra recorded from the isothermal adsorption. However, the desorbed CO_2 from the decomposition of carbonaceous species or the interaction of CO with lattice oxygen was favored at high temperature [21]. When CO adsorption was carried out at 298 K we were only able to detect the desorbed CO_2 in the temperature range 500–700 K on CuMnZrO_2 catalyst corresponding to decomposition of carbonaceous species. With the rise of adsorption temperature the peak at low temperature was observed and the intensity of the peak at high temperature also increased, which indicated the reaction between CO and catalysts was aggravated. However, iron could enhance the reaction between CO and the surface, as revealed by the TPD results of Fe-CuMnZrO_2 catalysts that had a more intense peak at low temperature contrasted to CuMnZrO_2 [22–24]. But the total amounts of CO_2 desorption was less than that on CuMnZrO_2 sample at corresponding conditions. It suggested that the presence of

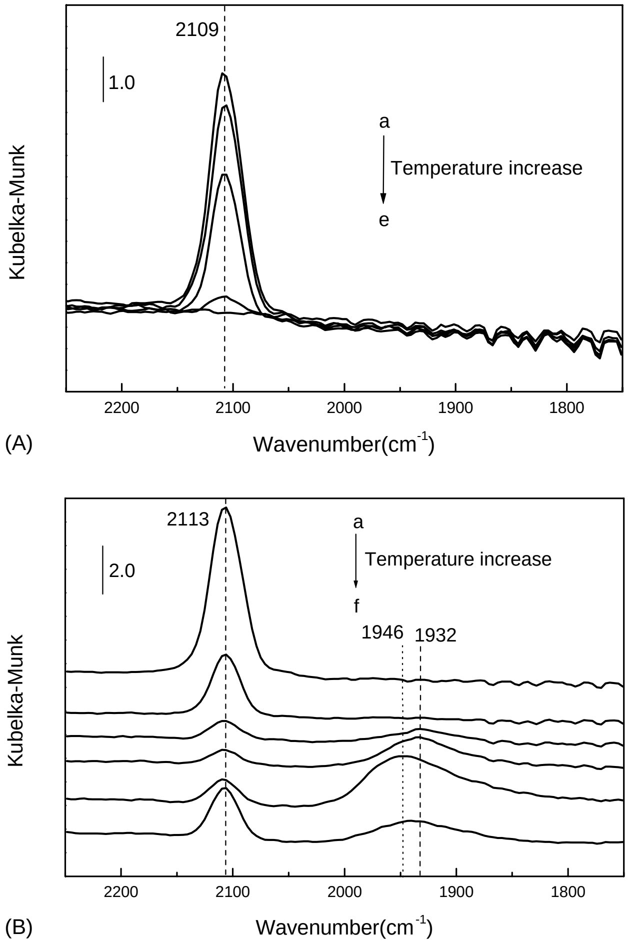

Fig. 5. Infrared spectra recorded from CO adsorption on $CuMnZrO_2$ (A) and Fe-$CuMnZrO_2$ (B) catalysts at different temperatures: (a) 298 K; (b) 323 K; (c) 373 K; (d) 473 K; (e) 573 K; (f) 623 K.

iron greatly influenced the formation of intermediate species on the catalyst surface.

3.4. Infrared spectra of CO adsorption

When CO adsorption on $CuMnZrO_2$ catalysts occurred at 298 K Only a single IR band at 2109 cm^{-1} was observed, corresponding to CO linearly adsorbed on copper species [25]. At higher temperature the peak for CO linearly adsorbed on copper decreased monotonically (see Fig. 5A). Compared with the spectra of CO adsorbed on $CuMnZrO_2$, more adsorption species could be discriminated over Fe-$CuMnZrO_2$. When CO adsorption occurred at 298 K, one peak at 2113 cm^{-1} was observed, also for linear CO species on copper sites (see Fig. 5B). It was noteworthy that the intensity of the band decreased with the rise of adsorption temperature and showed a minimum at 473 K then increased. In addition, two new bands at 1932 and 1946 cm^{-1} appeared after CO adsorption at 423 and 473 K, respectively. They reached a maximum at 573 K.

Based on the results above, one important issue should be clarified, that was, the CO adsorption properties of the copper were influenced consumingly by the addition of iron. In the infrared spectra of CO adsorbed on the $CuMnZrO_2$ catalyst, only one band at 2109 cm^{-1} was observed that corresponded to CO linearly adsorbed on copper sites. The band shifted to high frequency at 2113 cm^{-1} when iron was introduced into $CuMnZrO_2$ catalyst. This suggested that the interaction between copper and iron resulted in decrease of the antibonding of the copper d-electrons to the $2\pi^*$-orbital of the CO molecule, thus the carbon–copper bond in the chemisorbed CO molecule on copper sites was weakened, which led to the band of CO adsorbed shift to high frequency. Moreover, the intensity of the linear CO species on copper sites kept reducing on the $CuMnZrO_2$ catalyst with the increase of adsorption temperature because of the reconstruction and/or the poisoning (carbon deposition coming from the CO dissociation or disproportionation) of metal particles in the course of the CO adsorption [26]. While, for the Fe-$CuMnZrO_2$ catalyst, it showed a minimum at 473 K, suggesting that the presence of iron enhanced the intensity of the linear CO species on copper sites and influenced the process of carbon deposition.

On the other hand, two new broad bands at 1932 and 1946 cm^{-1} appeared at 423 and 473 K on the Fe-$CuMnZrO_2$ catalyst, respectively, and would reached maximum at 573 K. Compared with the spectra results of $CuMnZrO_2$ catalyst, we could draw a conclusion that the two bands were correspondent to the CO bridge-adsorbed on iron sites [27], which was in agreement with the findings of the CO-TPD study.

Huang and Anderson [28] reported that the reduction of hematite first to magnetite and then to iron followed the reactions:

$$\alpha Fe_2O_3 \xrightarrow{523\text{–}573\,K+H_2-H_2O} Fe_3O_4 \xrightarrow{673\,K+H_2-H_2O} \alpha Fe \tag{2}$$

Thus, the iron could not be reduced completely under the present condition at pretreated process. But the CO played an important role in the activation of iron. Indeed, it was found that the intensity of CO bridge-adsorbed on iron sites increased with the CO adsorption temperature. This indicated that the surface adsorption sites of iron were enhanced by CO. Usually the bridged-form CO was considered to be more active than the linear CO and favored to chain growth [29,30]. Therefore, the high activity of Fe-$CuMnZrO_2$ catalyst for higher alcohols synthesis seemed to be associated with the formation of bridge-type CO, which was easily dissociated to oxygen and carbon.

The IR bands between 1000 and 1700 cm^{-1} have been assigned to carbonaceous species on catalysts. It has been previously reported that on Cu/ZrO_2 catalysts system. Baiker and co-workers [10,12,31] have reported that for both CO and CO_2 hydrogenation on Cu/ZrO_2 for methanol synthesis, the CO adsorbed on the catalysts to form carbonate species, which then underwent hydrogenation to produce bidentate carbonate (b-$CO_3{}^{2-}$) or bicarbonate (b-$HOCOO_s{}^-$) or formate species (b-$HCOO_s{}^-$), then methoxy species (CH_3O_s),

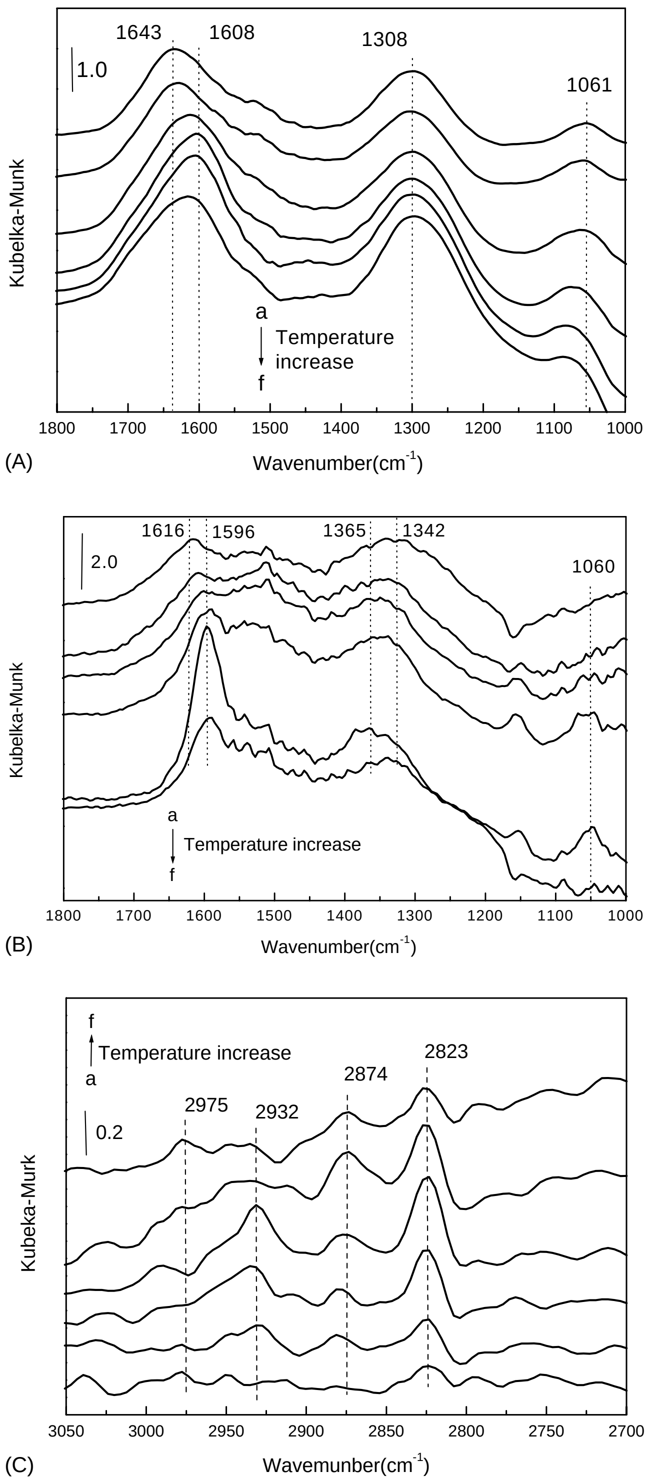

Fig. 6. Infrared spectra recorded from CO adsorption on $CuMnZrO_2$ (A) and Fe-$CuMnZrO_2$ (B and C) catalysts at different temperatures: (a) 298 K; (b) 323 K; (c) 373 K; (d) 473 K; (e) 573 K; (f) 623 K.

and finally methanol formation. The formation of intermediate species could be varied by doping different promoters, such as Zn, La, Cr and Mn. In the present case, for CO adsorbed on $CuMnZrO_2$ at 298 K, features attributed to b-CO_3^{2-} (1643 and 1292 cm^{-1}) [21], and CH_3O_s (1061, 2823 and 2932 cm^{-1}) [32] are prevalent (see Fig. 6A). The presence of CH_3O_s may be the result of the carbonaceous reacting with the hydrogen remaining on the catalyst surface after reduction, even though the catalyst was purged at 573 K for 30 min in Ar to removed adsorbed hydrogen. As adsorption temperature increased to 573 K the band for b-CO_3^{2-} decreased in intensity, while the predominant species present were b-$HOCOO_s^-$ (1608 and 1308 cm^{-1}) on the $CuMnZrO_2$ sample, at which temperature the $CuMnZrO_2$ catalyst had a top activity for methanol synthesis as reported in our previous papers [13,14], suggesting that b-$HOCOO_s^-$ was probably the precursor of methanol for $CuMnZrO_2$.

In contrast, for the iron promoted $CuMnZrO_2$ catalyst (see Fig. 6B), when CO adsorption occurred at 298 K the predominant features were bands at 1612 and 1342 cm^{-1}, which could be attributed to b-$HOCOO_s^-$. At higher temperature, significant bidentate formate (b-$HCOO_s^-$) formation became evident giving characteristic maxima at 1365, 1596, 2874 and 2975 cm^{-1} and the intensity of the bands went through a maximum at 573 K (see Fig. 6C). At about 373 K the features observable at 1060, 2823 and 2932 cm^{-1} was assigned to CH_3O_s and showed a maximum at 573 K. These results indicated that b-$HCOO_s^-$ was probably the precursor of methanol for Fe-$CuMnZrO_2$ catalyst. Therefore, the presence of iron influenced the formation of carbonaceous species and the process of the hydrogenation of carbonaceous species on the catalysts surface. This result was consistent with the TPD results, which demonstrated that the CO_2 from decomposition of carbonaceous species was varied in the presence of iron.

4. Conclusion

The interaction of CO with $CuMnZrO_2$ or Fe-$CuMnZrO_2$ catalysts were investigated by temperature-programmed desorption and in situ diffuse reflectance FTIR coupled with probe adsorption. It was found that the adsorption features of catalysts changed significantly with the addition of iron. On the one hand, the presence of iron improved the copper dispersion, which resulted in the total adsorption of CO increase, and intensified the reaction between CO and catalyst surface. Moreover, the CO adsorbed on iron sites was detected in FTIR and TPD study, and was considered to be more active than CO adsorbed on copper and favored to chain growth in hydrogenation. In addition, the CO played an important role in the activation of iron. On the other hand, the presence of iron influenced the formation of carbonaceous species and changed the process of the hydrogenation of carbonaceous species on the catalysts surface. Bidentate carbonate species formed on the $CuMnZrO_2$ sample when CO adsorption took place at 298 K and bicarbonate species at 573 K, while bicarbonate and formate species formed on the Fe-$CuMnZrO_2$ catalyst at same conditions, respectively. Thus, the presence of iron greatly influenced the process of methanol synthesis. The effect of iron will be reflected by the $C_2{}^+OH$ formation and by-production formation in higher alcohols synthesis.

Acknowledgements

This work was supported by the State Key Foundation Project for Development and Research of China (G1999022400) and Knowledge Innovation Program of CAS (KGCX2-302).

References

[1] X.D. Xu, E.B.M. Doesberg, J.J.F. Scholten, Catal. Today 2 (1987) 125.
[2] A. Kiennemann, C. Diagne, J.P. Hindermann, Appl. Catal. 53 (1989) 197.
[3] G.J.J. Bartley, R. Burch, Appl. Catal. 43 (1988) 141.
[4] Y. Sun, P.A. Sermon, J. Chem. Soc. Chem. Commun. (1993) 1242.
[5] R.G. Silver, N.B. Jachson, Y.G. Ekerdt, in: W.M. Ayers (Ed.), Catalytic Activation of Carbon Dioxide, ACS Symposium Series 363, American Chemical Society, Washington, DC, 1988, p. 123 and references therein.
[6] E. Guglielminetti, Langmuir 6 (1990) 1445.
[7] G.C. Chinchen, M.S.S. Spencer, Catal. Today 10 (1991) 293.
[8] S.G. Neophytides, A.J. Marchi, G.F. Froment, Appl. Catal. A 86 (1992) 45.
[9] M. Bowker, R.A. Hadden, H. Houghton, J.N.K. Hyland, K.C. Waugh, J. Catal. 109 (1988) 263.
[10] C. Schild, A. Wokaun, A. Baiker, J. Mol. Catal. 63 (1990) 223.
[11] C. Schild, A. Wokaun, A. Baiker, J. Mol. Catal. 63 (1990) 243.
[12] J. Weigel, R.A. Koeppel, A. Baiker, A. Wokaun, Langmuir 12 (1996) 5319.
[13] Y. Sun, X. Chen, X. Wang, J. Ren, B. Zhong, CN Patent, 98104989 (1998).
[14] Y. Sun, X. Chen, B. Zhong, X. Wang, J. Ren, CN Patent, 98118954 (1998).
[15] N. Zhao, R. Xu, W. Wei, Y. Sun, React. Kinet. Catal. Lett. 75 (2002) 297.
[16] R. Xu, Z. Ma, C. Yang, W. Wei, Y. Sun, Preprints of American Chemical Society, Division of Fuel Chemistry 48 (2003) 217.
[17] R. Xu, Z. Ma, C. Yang, W. Wei, Y. Sun, React. Kinet. Catal. Lett. 81 (2004) 91.
[18] J.W. Evans, M.S. Wainwright, A.J. Bridgewater, D.J. Youny, Appl. Catal. 7 (1983) 75.
[19] W.R.A.M. Robinson, J.C. Mol, Appl. Catal. 98 (1993) 81.
[20] D. Bianchi, T. Chafik, M. Khalfallah, S.J. Teichner, Appl. Catal. A 112 (1994) 57.
[21] D. Bianchi, T. Chafik, M. Khalfallah, S.J. Teichner, Appl. Catal. A 105 (1993) 223.
[22] T.J. Huang, T.C. Yu, S.H. Chang, Appl. Catal. 52 (1989) 157.
[23] C. Serre, F. Garin, G. Belot, G. Maire, J. Catal. 141 (1993) 1.
[24] J. Venter, M. Kaminsky, G.L. Geoffroy, M.A. Vannice, J. Catal. 103 (1987) 450.
[25] I.A. Fisher, A.T. Bell, J. Catal. 178 (1998) 153.
[26] T. Chafik, O. Dulaurent, J.L. Gass, D. Bianchi, J. Catal. 179 (1998) 503.
[27] N. Sheppard, T.T. Nguyen, in: R.J.H. Clark, R.E. Hester (Eds.), Advances in Infrared and Raman Spectroscopy, vol. 5, 1978, p. 67.
[28] J.J. Huang, J.R. Anderson, J. Catal. 40 (1975) 143.
[29] N. Tsubaki, S.L. Sun, K. Fujimoto, J. Catal. 199 (2001) 236.
[30] J.P. Hindermann, G.J. Hutchings, A. Kiennemann, Cat. Rev.-Sci. Eng. 35 (1993) 1.
[31] A. Baiker, M. Kilo, M. Maciejewski, S. Menzi, A. Wokaun, in: L. Guczi, et al. (Eds.), New Frontiers in Catalysis, Proceedings of the 10th International Congress on Catalysis, Elsevier, Amsterdam, 1993, p. 1257.
[32] D.B. Clarke, D.K. Lee, M.J. Sandoval, A.T. Bell, J. Catal. 150 (1994) 81.